Article

Functional One-Dimensional Lipid Bilayers on Carbon Nanotube Templates

Alexander B. Artyukhin, Aleksei Shestakov, Jennifer Harper, Olgica Bakajin, Pieter Stroeve, and Aleksandr Noy

J. Am. Chem. Soc., **2005**, 127 (20), 7538-7542• DOI: 10.1021/ja043431g • Publication Date (Web): 30 April 2005

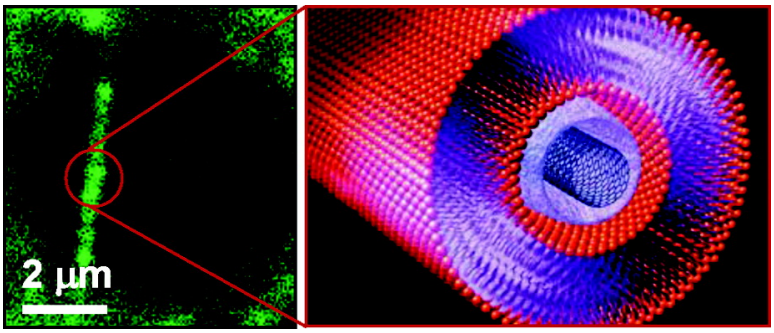

More About This Article

Additional resources and features associated with this article are available within the HTML version:

- Supporting Information
- Links to the 10 articles that cite this article, as of the time of this article download
- Access to high resolution figures
- Links to articles and content related to this article
- Copyright permission to reproduce figures and/or text from this article

View the Full Text HTML

J|A|C|S
ARTICLES
Published on Web 04/30/2005

Functional One-Dimensional Lipid Bilayers on Carbon Nanotube Templates

Alexander B. Artyukhin,[†,‡] Aleksei Shestakov,[§] Jennifer Harper,[†] Olgica Bakajin,[†] Pieter Stroeve,[‡] and Aleksandr Noy*[,†]

Contribution from the Biosecurity and Nanosciences Laboratory, Chemistry and Materials Science Directorate, Lawrence Livermore National Laboratory, 7000 East Avenue, Livermore, California 94550, Department of Chemical Engineering and Materials Science, University of California, Davis, California 95616, and AX Division, Lawrence Livermore National Laboratory, 7000 East Avenue, Livermore, California 94550

Received October 29, 2004; E-mail: noy1@llnl.gov

Abstract: Use of biological machines and environments in novel bioinorganic nanostructures is critical for development of new types of biosensors, bio-NEMS devices, and functional materials. Lipid bilayers that mimic a cell membrane have already played an important role in such applications. We present supported lipid bilayers that spontaneously assemble in a continuous nanoshell around a template of a carbon nanotube wrapped with hydrophilic polymer cushion layers. We demonstrate that such 1-D lipid membranes are fluid and can heal defects, even over repeated damage−recovery cycles. A simple diffusion model can describe mobility of lipid molecules in these 1-D nanoshells. These structures could lead to the development of new classes of biosensors and bioelectronic devices.

Introduction

Unique structural, mechanical, and electronic properties of carbon nanotubes have catalyzed many important discoveries in physics, chemistry, and materials science.[1,2] To achieve a similar success with biophysical applications, we must overcome the challenge of integrating these materials with key biological machines and environments. We also must come up with fabrication strategies for using biological components in novel structures that facilitate device applications. Graphitic surface of a naked carbon nanotube is extremely resistant to any functional coupling of biological molecules and exhibits a high degree of nonspecific adhesion, which is detrimental to the real-world performance of any device. Researchers have demonstrated noncovalent modification of carbon nanotubes with polymers,[3−5] proteins,[6] specific peptides,[7] DNA sequences,[8] and monolayers of amphiphilic molecules.[9] However, most of these coatings provide at best only a chemical "anchor" for a biological machine without any additional capability to orient the molecule or facilitate its function. In contrast, natural systems often use lipid membranes as a universal host matrix[10] that can support a large number of membrane proteins and receptors that perform a host of functions ranging from ion transport[11] to signal transduction.[12] Functionalization of carbon nanotubes with lipid bilayers should provide a robust and general strategy for using membrane proteins in nanodevices. Lipid bilayers are virtually impermeable to ions and large molecules,[13−15] providing a natural barrier to nonspecific adsorption.

Although lipid bilayers in two-dimensional (2-D) planar geometries[16] as well as quasi-zero-dimensional (0-D) geometries[17,18] are well-known, common phospholipids do not spontaneously form 1-D tubular structures in aqueous solutions unless they are forced into a metastable configuration by an

[†] Biosecurity and Nanosciences Laboratory, Lawrence Livermore National Laboratory.
[‡] University of California Davis.
[§] AX Division, Lawrence Livermore National Laboratory.

(1) Baughman, R. H.; Zakhidov, A. A.; de Heer, W. A. *Science* **2002**, *297*, 787−792.
(2) Ouyangl, M.; Huang, J. L.; Lieber, C. M. *Acc. Chem. Res.* **2002**, *35*, 1018−1025.
(3) Shim, M.; Kam, N. W. S.; Chen, R. J.; Li, Y. M.; Dai, H. J. *Nano Lett.* **2002**, *2*, 285−288.
(4) O'Connell, M. J.; Boul, P.; Ericson, L. M.; Huffman, C.; Wang, Y. H.; Haroz, E.; Kuper, C.; Tour, J.; Ausman, K. D.; Smalley, R. E. *Chem. Phys. Lett.* **2001**, *342*, 265−271.
(5) Star, A.; Stoddart, J. F.; Steuerman, D.; Diehl, M.; Boukai, A.; Wong, E. W.; Yang, X.; Chung, S. W.; Choi, H.; Heath, J. R. *Angew. Chem., Int. Ed.* **2001**, *40*, 1721−1725.
(6) Chen, R. J.; Bangsaruntip, S.; Drouvalakis, K. A.; Kam, N. W. S.; Shim, M.; Li, Y. M.; Kim, W.; Utz, P. J.; Dai, H. J. *Proc. Natl. Acad. Sci. U.S.A.* **2003**, *100*, 4984−4989.
(7) Wang, S. Q.; Humphreys, E. S.; Chung, S. Y.; Delduco, D. F.; Lustig, S. R.; Wang, H.; Parker, K. N.; Rizzo, N. W.; Subramoney, S.; Chiang, Y. M.; Jagota, A. *Nat. Mater.* **2003**, *2*, 196−200.
(8) Zheng, M.; Jagota, A.; Semke, E. D.; Diner, B. A.; McLean, R. S.; Lustig, S. R.; Richardson, R. E.; Tassi, N. G. *Nat. Mater.* **2003**, *2*, 338−342.
(9) Richard, C.; Balavoine, F.; Schultz, P.; Ebbesen, T. W.; Mioskowski, C. *Science* **2003**, *300*, 775−778.
(10) Alberts, B.; Bray, D.; Lewis, J.; Raff, M.; Roberts, K.; Watson, J. D. *Molecular Biology of the Cell*; Garland Publishing: New York, 1994.
(11) Aidley, D. J.; Stanfield, P. R. *Ion Channels: Molecules in Action*; Cambridge University Press: New York, 1996.
(12) Gomperts, B. D.; Kramer, I. M.; Tatham, P. E. R. *Signal Transduction*; Academic Press: New York, 2002.
(13) Tien, H. T.; Ottova-Leitmannova, A. L. *Planar Lipid Bilayers (BLMs) and Their Applications*; Elseiver Science: New York, 2003.
(14) Katsaras, J.; Gutberlet, T. *Lipid Bilayers: Structure and Interactions*; Springer-Verlag: New York, 2001.
(15) Walter, A.; Gutknecht, J. *J. Membr. Biol.* **1986**, *90*, 207−217.
(16) Sackmann, E. *Science* **1996**, *271*, 43−48.
(17) Lasic, D. D. *Liposomes: From Physics to Applications*; Elsevier: Amsterdam, 1993.
(18) Major, M.; Prieur, E.; Tocanne, J. F.; Betbeder, D.; Sautereau, A. M. *Biochim. Biophys. Acta* **1997**, *1327*, 32−40.

10.1021/ja043431g CCC: $30.25

external force.[19−21] Cylindrical lipid tubes ranging from 20 to 500 nm in diameter can also form spontaneously when the structure and shape of lipid molecules are carefully designed, such as in case of galactosylceramides[22,23] and diacetylenic lipids.[24] Researchers have also observed lipid tubules in biological systems both in vivo[25−27] and in vitro.[28−31]

We propose and demonstrate spontaneous self-assembly of common phospholipids into tubular one-dimensional geometry by using carbon nanotubes as assembly templates. In our experiments, we modify the nanotube surface with hydrophilic polymer layers and then assemble a continuous lipid bilayer shell around this structure. We demonstrate that the lipid membrane maintains its fluidity in 1-D geometry, and that the mobility of lipid molecules can still be described by a simple diffusion model. Our structures are highly robust and can sustain repeated damage−recovery cycles. These properties should enable development of a range of functional bioinorganic nanostructures based on 1-D lipid bilayers.

Materials and Methods

Materials. Most of the reagents used in this study were available commercially and used as received. Copper transmission electron microscope bare grids (2000 mesh) were obtained from Ted Pella, Inc.

Nanotube Preparation and Polymer Adsorption. We used bare TEM grids as a substrate to grow suspended carbon nanotubes. Details of the nanotube synthesis and subsequent polymer adsorption were described in a recent publication.[32] For this work, we have significantly improved the rinsing procedure between adsorption steps by using simultaneous injection and withdrawal of liquid (50−100 mL) with two syringe pumps. We held the sample in a 2 mL beaker and continuously stirred solution during adsorption and rinsing. Polymers were adsorbed from 50 mM solutions (concentration of monomer units) with no added salt.

Lipid Bilayer Formation. We used ultrasonication to prepare lipid vesicles composed of 1-stearoyl-2-oleoyl-*sn*-glycero-3-[phospho-L-serine] sodium salt (SOPS), 1-palmitoyl-2-oleoyl-*sn*-glycero-3-phosphocholine (POPC), and 2-(4,4-difluoro-5-methyl-4-bora-3a,4a-diaza-s-indacene-3-do-decanoyl)-1-hexadecanoyl-*sn*-glycero-3-phosphocholine (BODIPY-PC) in the ratio 75:23:2 (SOPS:POPC:BODIPY-PC) following a previously described procedure.[33] The grid with polymer-coated carbon nanotubes was incubated with vesicles for 40−50 min. We previously found this time to be sufficient to reach equilibrium for bilayer formation on a flat substrate.[33]

Fluorescence Confocal Microscopy and Fluoresence Recovery After Photobleaching (FRAP) Experiments. After the preparation steps were completed, we placed the grid in a thin water layer between two clean glass cover slips for fluorescent imaging. Thin liquid film remaining between the cover slips was able to keep the grid with lipid-coated nanotubes in aqueous environment for days. Design of our laser scanning confocal microscope was described earlier.[34] All fluorescence images were collected using 100X (1.4 NA) Plan Apo oil-immersion objective (Nikon). We used 488 nm line of Ar-ion laser (Coherent Innova 70) for BODIPY-PC excitation. Collected optical signal first passed through a long-pass filter (Chroma Technology) to reject excitation light and then was focused onto a single photon counting module (Perkin-Elmer Optoelectronics). All images were acquired using NanoscopeIII SPM controller (Veeco-DI).

For FRAP experiments, we used a high-intensity beam (ca. 50 μW) of our confocal microscope to bleach out a small region (0.5 μm) in the center of the coated nanotube. We then monitored the recovery of the fluorescence intensity (detected as the maximum of the emission spectrum) in the same area using much weaker excitation intensity (ca. 1 μW). Site-resolved spectroscopy was performed with a SpectraPro 300i spectrometer equipped with a back-illuminated, liquid nitrogen-cooled CCD camera (Roper Scientific).

Transmission Electron Microscopy. Analysis was performed on a Philips CM300 FEG transmission electron microscope, operating at 300 kV, and utilizing a Gatan imaging filter.

Results and Discussion

Substrate Design. Direct assembly of lipid bilayers on carbon nanotubes is challenging. Typical diameters of single-wall carbon nanotubes range from 1 to 5 nm, which is well below the smallest reported lipid bilayer curvature.[35] More important, hydrophobic nanotube surface does not support the polar headgroups of a lipid bilayer; instead, it produces a monolayer of lipids with hydrophobic tails in direct contact with the nanotube.[9,36] To support a lipid *bilayer*, the nanotube surface must bear a hydrophilic cushion layer. Recently, we demonstrated controlled modification of nanotube surfaces using layer-by-layer self-assembly of polyelectrolytes.[32] Polyelectrolyte multilayers are well-known substrates for supported lipid bilayers[33,37−43] and are ideal for providing the hydrophilic support. Polyelectrolyte cushion layer not only separates the bilayer from a hydrophobic nanotube surface but also provides additional stabilization due to the electrostatic interactions of the lipid headgroups with the oppositely charged polymer. In addition, the number of polymer layers controls the polymer cushion thickness, which allows us to match the diameter of the support to the critical curvature of the lipid bilayer.

Our experiments concentrated on functionalizing nanotubes suspended between solid supports because this configuration

(19) Evans, E.; Bowman, H.; Leung, A.; Needham, D.; Tirrell, D. *Science* **1996**, *273*, 933−935.
(20) Roux, A.; Cappello, G.; Cartaud, J.; Prost, J.; Goud, B.; Bassereau, P. *Proc. Natl. Acad. Sci. U.S.A.* **2002**, *99*, 5394−5399.
(21) Karlsson, A.; Karlsson, R.; Karlsson, M.; Cans, A. S.; Stroemberg, A.; Ryttsen, F.; Orwar, O. *Nature* **2001**, *409*, 150−152.
(22) Kulkarni, V. S.; Anderson, W. H.; Brown, R. E. *Biophys. J.* **1995**, *69*, 1976−1986.
(23) Wilson-Kubalek, E. M.; Brown, R. E.; Celia, H.; Milligan, R. A. *Proc. Natl. Acad. Sci. U.S.A.* **1998**, *95*, 8040−8045.
(24) Schnur, J. M. *Science* **1993**, *262*, 1669−1676.
(25) Cluett, E. B.; Wood, S. A.; Banta, M.; Brown, W. J. *J. Cell Biol.* **1993**, *120*, 15−24.
(26) Sciaky, N.; Presley, J.; Smith, C.; Zaal, K. J. M.; Cole, N.; Moreira, J. E.; Terasaki, M.; Siggia, E.; Lippincott-Schwartz, J. *J. Cell Biol.* **1997**, *139*, 1137−1155.
(27) Rustom, A.; Saffrich, R.; Markovic, I.; Walther, P.; Gerdes, H. H. *Science* **2004**, *303*, 1007−1010.
(28) Takei, K.; Haucke, V.; Slepnev, V.; Farsad, K.; Salazar, M.; Chen, H.; De Camilli, P. *Cell* **1998**, *94*, 131−141.
(29) Takei, K.; Slepnev, V.; Haucke, V.; De Camilli, P. *Nat. Cell Biol.* **1999**, *1*, 33−39.
(30) Stowell, M. H. B.; Marks, B.; Wigge, P.; McMahon, H. T. *Nat. Cell Biol.* **1999**, *1*, 27−32.
(31) Farsad, K.; Ringstad, N.; Takei, K.; Floyd, S. R.; Rose, K.; De Camilli, P. *J. Cell Biol.* **2001**, *155*, 193−200.
(32) Artyukhin, A. B.; Bakajin, O.; Stroeve, P.; Noy, A. *Langmuir* **2004**, *20*, 1442−1448.
(33) Zhang, L. Q.; Longo, M. L.; Stroeve, P. *Langmuir* **2000**, *16*, 5093−5099.
(34) Noy, A.; Huser, T. R. *Rev. Sci. Instrum.* **2003**, *74*, 1217−1221.
(35) Huang, C.; Mason, J. T. *Proc. Natl. Acad. Sci. U.S.A.* **1978**, *75*, 308−310.
(36) O'Connell, M. J.; Bachilo, S. M.; Huffman, C. B.; Moore, V. C.; Strano, M. S.; Haroz, E. H.; Rialon, K. L.; Boul, P. J.; Noon, W. H.; Kittrell, C.; Ma, J. P.; Hauge, R. H.; Weisman, R. B.; Smalley, R. E. *Science* **2002**, *297*, 593−596.
(37) Cassier, T.; Sinner, A.; Offenhauser, A.; Mohwald, H. *Colloids Surf., B* **1999**, *15*, 215−225.
(38) Kugler, R.; Knoll, W. *Bioelectrochem.* **2002**, *56*, 175−178.
(39) Ma, C.; Srinivasan, M. P.; Waring, A. J.; Lehrer, R. I.; Longo, M. L.; Stroeve, P. *Colloids Surf., B* **2003**, *28*, 319−329.
(40) Moya, S.; Donath, E.; Sukhorukov, G. B.; Auch, M.; Baumler, H.; Lichtenfeld, H.; Mohwald, H. *Macromolecules* **2000**, *33*, 4538−4544.
(41) Moya, S. E.; Georgieva, R.; Baumler, H.; Richter, W.; Donath, E. *Med. Biol. Eng. Comput.* **2003**, *41*, 504−508.
(42) Tiourina, O. P.; Radtchenko, I.; Sukhorukov, G. B.; Mohwald, H. *J. Membr. Biol.* **2002**, *190*, 9−16.
(43) Wong, J. Y.; Majewski, J.; Seitz, M.; Park, C. K.; Israelachvili, J. N.; Smith, G. S. *Biophys. J.* **1999**, *77*, 1445−1457.

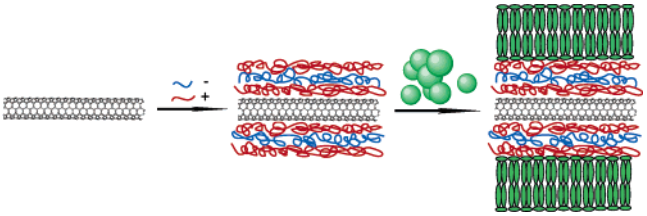

Figure 1. Schematics of polymer and lipid assembly on carbon nanotubes. First, carbon nanotubes are coated with several alternating layers of oppositely charged polyelectrolytes, followed by the formation of lipid bilayer by vesicle fusion.

allowed us to form a continuous lipid bilayer around the nanotube circumference. We started our assembly process (Figure 1) by modifying pristine suspended single-wall carbon nanotubes with five alternating polymer layers composed of strong polyelectrolytes, such as poly(diallyldimethylammonium chloride) (PDDA), sodium poly(styrenesulphonate) (PSS), and poly(allylamine hydrochloride) (PAH).[32] The critical (i.e., smallest) inner radius of the lipid bilayer is ca. 5 nm.[35,44] Polyelectrolytes that form our cushion produce 1 nm thick layers at low ionic strength conditions;[45,46] therefore, we used five polymer layers to match the critical curvature of the bilayer. TEM images show that five alternating PAH/PSS layers produce smooth coating on the nanotubes over large distances (Figure 2A−E), with the diameter of the final structure of 10−15 nm (Figure 2D,E). Substitution of PAH to PDDA produces rougher coating of 10−30 nm in diameter (Figure 2F,G). Overall, the addition of the polymer cushion made the size of our nanotubes comparable (and in some cases even larger) to the smallest reported nanoparticles (14 nm) that can support lipid bilayers.[47]

1-D Bilayer Formation. We created supported lipid bilayers on our "cushioned" carbon nanotubes using vesicle fusion, which already is a proven technique for creating lipid bilayer on flat substrates.[48] We terminated the multilayer polymer cushion on nanotubes with a cationic layer (PDDA or PAH) to stabilize the bilayer that contains 75% of the anionic lipid (SOPS). To enable visualization of the final structure, the vesicles incorporated a small fraction of a fluorescent lipid probe (BODIPY-PC). Scanning confocal microscope images of the resulting structures show linear fluorescent features inside the holes of the TEM grid (Figure 3), which correspond to the lipid-coated carbon nanotubes stretching across the grid holes. These results indicate that partial strain relief in the dimension of the nanotube axis coupled with the electrostatic attraction of the bilayer to the polymer support is sufficient to stabilize the bilayer in 1-D configuration. We also argue that incorporation of charged lipids in the membrane should reject subsequent lipid multilayer formation. We and others have observed similar behavior experimentally for bilayers adsorbed on flat substrates;[33,39] therefore, we assume that our experiments produced a single bilayer on polymer-coated carbon nanotubes.

Lipid Diffusion in 1-D Bilayers. One of the most important features of a *functional* lipid bilayer is the ability of the lipid molecules to diffuse along the bilayer plane. To prove that our bilayers keep this property and to verify the bilayer continuity, we used FRAP to study mobility of the lipid molecules.[49] A

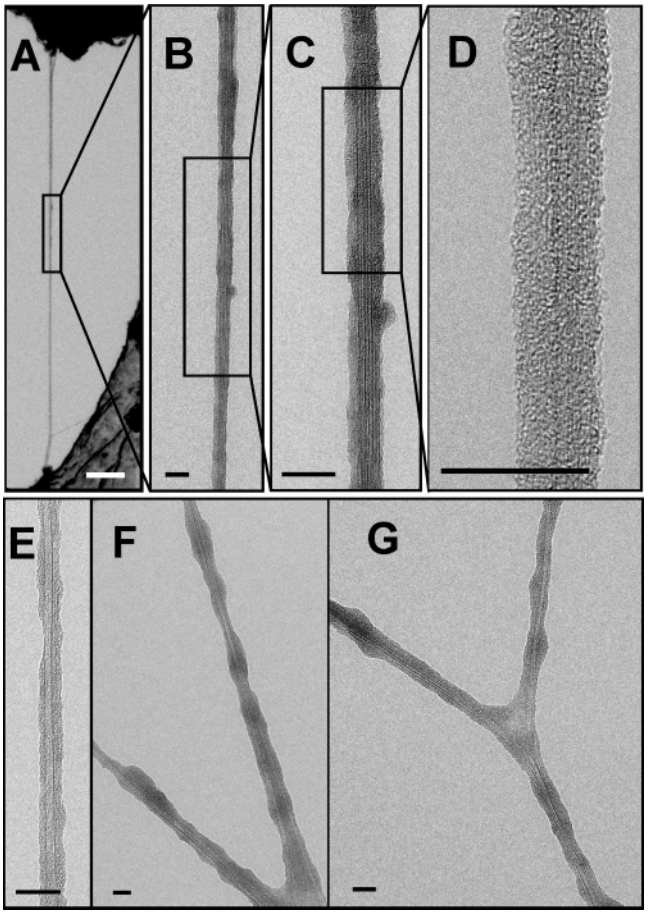

Figure 2. TEM images of carbon nanotubes after coating with five alternating PAH/PSS (A−E) or PDDA/PSS (F, G) layers. Scale bars: 200 nm (A), 20 nm (B−G).

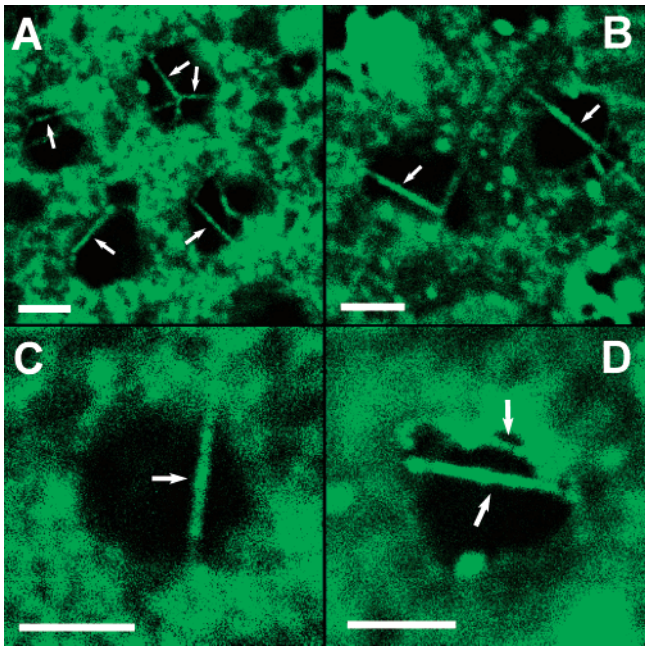

Figure 3. Confocal fluorescence images of TEM grids with carbon nanotubes coated with five polyelectrolyte layers and lipid bilayer. Polymer multilayer is composed of PAH/PSS (A−C) or PDDA/PSS (D). Visible nanotubes are indicated with arrows. Scale bars: 5 μm.

(44) Israelachvili, J. N.; Marcelja, S.; Horn, R. G. *Q. Rev. Biophys.* **1980**, *13*, 121−200.
(45) Dubas, S. T.; Schlenoff, J. B. *Macromolecules* **1999**, *32*, 8153−8160.
(46) Losche, M.; Schmitt, J.; Decher, G.; Bouwman, W. G.; Kjaer, K. *Macromolecules* **1998**, *31*, 8893−8906.
(47) Decuyper, M.; Joniau, M. *Eur. Biophys. J.* **1988**, *15*, 311−319.
(48) Brian, A. A.; McConnell, H. M. *Proc. Natl. Acad. Sci. U.S.A.* **1984**, *81*, 6159−6163.

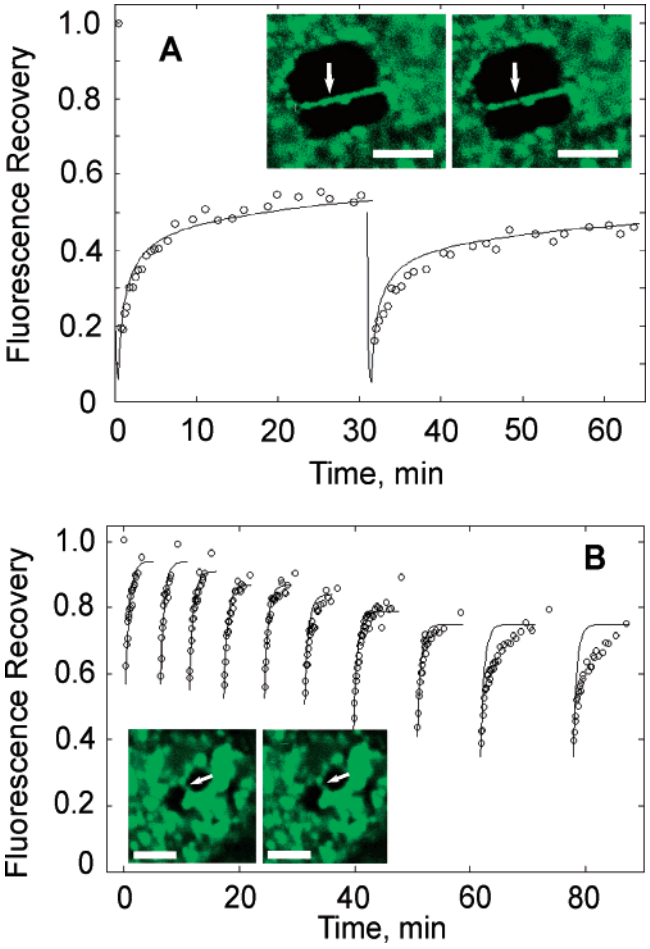

Figure 4. Experimental (dots) and model (line) fluorescence recovery curves during 2 (A) and 10 (B) FRAP cycles on the same spot on lipid-coated nanotubes. The polymer "cushion" is composed of PDDA and PSS. Parameters of the fit (see main text for full details): (A) $t_l = 30$ s, $R = 0.25\ s^{-1}$, $X = 7\ \mu m$, $D = 4 \times 10^{-3}\ \mu^2/s$. (B) $t_l = 30$ s in first 6 cycles, 1 min in 7th and 8th cycles, 2 min in 9th and 10th cycles, $R = 0.1\ s^{-1}$, $X = 0.8\ \mu m$, $D = 2 \times 10^{-3}\ \mu^2/s$. Left (right) insets on A and B show fluorescence images before first bleaching (after last recovery). Lipid-coated nanotubes are indicated with arrows. Scale bars: 5 μm.

large percentage of our 1-D lipid bilayers showed recovery of the fluorescence signal in the range of 20−90% with the average recovery level of about 50%, often sustaining multiple bleach−recovery cycles in the same spot (Figure 4). Figure 4A shows an example of two such cycles, which show recovery to an almost identical level. Some lipid-coated nanotubes were even able to sustain recovery over 10 bleaching cycles (Figure 4B). These results demonstrate that our lipid coating on the carbon nanotube is continuous, with the lipid molecules keeping their mobility even in these high-curvature structures. We also note that at least some of our lipid coatings showed high mobile fraction percentage (up to 90%), which indicates high quality of the bilayer in these samples. Bilayer quality is an important property[50] for future electronic applications of our systems, and further refinement may be necessary to achieve truly defect-free 1-D membranes.

We can further characterize lipid mobility in 1-D bilayers by using a quantitative model of the bleaching and recovery process. A rigorous model of this process must consider diffusion in a tubular structure. However, we note that in our experiments, the size of the bleaching spot (ca. 500 nm) is much larger than the lipid tubule diameter. Therefore, we can assume that we are always bleaching the lipid molecules along the circumference of the tube uniformly and model the problem as a simple one-dimensional diffusion (Figure 5). The normalized concentration of mobile fluorescent lipid molecules along the nanotube, $u(x, t)$, can be then described by the following equation where the first term describes diffusion and the second term describes photobleaching:

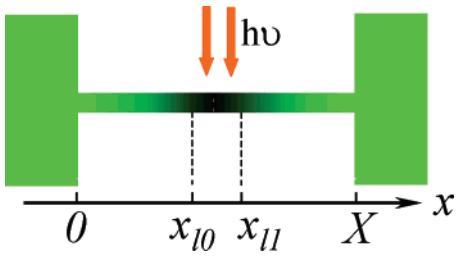

Figure 5. Schematics of the diffusion problem.

$$\partial_t u = \partial_x (D\, \partial_x u) - R(x, t)\, u \qquad (1)$$

Initially, the lipid is distributed uniformly along the nanotube:

$$u|_{t=0} = 1 \qquad (2)$$

Experimentally observed fluorescence is proportional to the total amount of fluorescent molecules within the collection spot:

$$U(t) = \int_{x_{l0}}^{x_{l1}} u(x, t)\, dx \qquad (3)$$

The boundary conditions describe lipid molecules' behavior at the nanotube junction with the support. Fluorescence images shown in Figure 3 indicate that lipid coverage extends onto the TEM grid support. This configuration can lead to two different boundary conditions. The bilayers on the nanotube and the grid could be isolated from each other, and the only source for fluorescence recovery would be unbleached species remaining on the nanotube. Alternatively, if the two bilayers are connected, the bilayer on the grid can act as an inexhaustible reservoir to support the recovery of the bilayer on the nanotube. In general, the diffusion kinetics should be weakly sensitive to the boundary conditions for the longer nanotube. The boundary conditions will play a much more important role for shorter nanotubes, where the nanotube length is comparable to the diffusion distance over bleaching time or to the size of the bleaching spot. For our data, the isolated boundary condition produces reasonable fits for long nanotubes; however, it fails to provide good fit for recovery kinetics on short nanotubes. In contrast, the transparent boundary condition produces excellent fit for both long (Figure 4A) and short (Figure 4B) nanotubes. Multiple bleaching recovery cycles provide an additional argument for the existence of the connection between bilayers on the nanotube and the grid. If the nanotube bilayer were isolated, most of fluorescent molecules on a short nanotube (Figure 4B) would be bleached out during the first few cycles given our relatively long bleaching times (0.5−2 min) and fast recovery. Interestingly, the last two recovery cycles in Figure 4B show large deviation from the behavior predicted by the model, which may indicate that we started depleting the lipid reservoir on the grid.

(49) Axelrod, D.; Koppel, D. E.; Schlessinger, J.; Elson, E.; Webb, W. W. *Biophys. J.* **1976**, *16*, 1055−1069.
(50) Wiegand, G.; Arribas-Layton, N.; Hillebrandt, H.; Sackmann, E.; Wagner, P. *J. Phys. Chem. B* **2002**, *106*, 4245−4254.

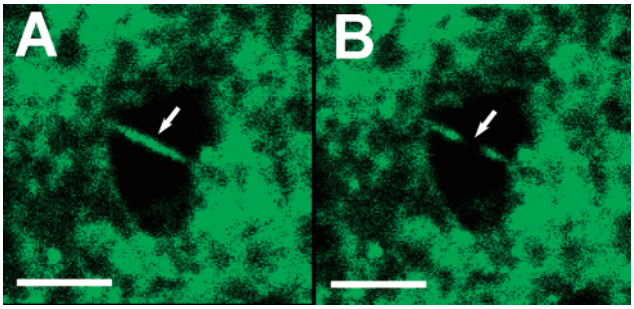

Figure 6. Confocal fluorescence images of TEM grids with carbon nanotubes coated with five PAH and PSS layers and lipid bilayer before (A) and after (B) bleaching. The nanotubes are indicated with arrows. Scale bars: 5 μm.

Lipid mobility in our 1-D bilayers ($2-4 \times 10^{-3}$ μ^2/s) is about 3 orders of magnitude lower than lipid mobility in fluid bilayers adsorbed on glass ($1-5$ μ^2/s).[51] However, it falls near the lower limit of the reported range for polyelectrolyte-supported lipid membranes[37,38,52] (which almost always show mobility at least an order of magnitude lower than bilayers supported on glass). Notably, our 1-D bilayers showed a mobility almost 2 orders of magnitude lower than that of the bilayers of the same lipid composition supported on the same polymer cushion on a flat substrate ($0.1-0.2$ μ^2/s).[33,39] Higher defect density in lipid membranes on nanotubes compared to that of the flat bilayers might lead to obstructed diffusion[53] and effectively decrease diffusion coefficients.

Interestingly, the lipid mobility in our structures can depend dramatically on the composition of the polymer cushion. A large percentage of 1-D bilayers supported on a PDDA/PSS polymer cushion showed recovery after bleaching. In these cases, fluorescent images of the nanotubes before bleaching and after recovery were almost undistinguishable (Figure 4A,B, insets). However, the same lipid membrane supported on nanotubes with PAH/PSS polymer cushion was immobile on the time scale of our experiment, clearly showing a bleached spot on a lipid-coated nanotube in the fluorescence image (Figure 6). This behavior indicates that the lipid headgroups interact stronger with PAH layer than with PDDA layer, which is consistent with stronger coupling in PAH/PSS multilayers compared to PDDA/PSS multilayers.[54,55] We can attribute these effects to higher linear charge density of PAH and the presence of hydrogen bonding primary amine groups in PDDA structure. Two bulky methyl groups may also further screen the charge center in PDDA.

Conclusions

We showed that lipid bilayers can spontaneously wrap around single-wall carbon nanotubes modified with a multilayer polyelectrolyte "cushion". Such cushion provided a hydrophilic support surface to maintain the bilayer structure. Fluorescence recovery after photobleaching experiments showed that the lipid molecules in our bilayers are laterally mobile despite the high bilayer strain in these nanostructures. We also showed that the bilayers are robust enough to sustain multiple bleaching−recovery cycles.

We believe that our structures open up significant new possibilities for chemists, biologists, and materials scientists. Our system provides the opportunity to test the ultimate physical limits of bilayer self-assembly in a highly controlled and fully tunable system. Moreover, strong coupling of the lipid mobility to the properties of the underlying substrate gives us the ability to fine-tune the diffusion properties of our 1-D bilayers.

Lipid membranes provide an efficient and biocompatible barrier between the nanotube surface and the surrounding solution. Reconstitution of the membrane protein channels into the 1-D bilayers should provide a robust way to control and modulate access of the small molecules to the nanotube surface. Controlled reconstitution of other types of proteins into the lipid bilayers could enable controlled assembly of more complex nanostructures. Finally, lipid-coated nanotubes could be used as biocompatible probes of intracellular environments or as a structural foundation for hybrid bioinorganic nanostructures.

Acknowledgment. A.A. acknowledges an SEGR Fellowship from LLNL. This work was performed under the auspices of the U.S. Department of Energy by the University of California, Lawrence Livermore National Laboratory, under Contract No. W-7405-Eng-48.

JA043431G

(51) Tocanne, J. F.; Dupoucezanne, L.; Lopez, A. *Prog. Lipid Res.* **1994**, *33*, 203−237.
(52) Auch, M.; Fischer, B.; Mohwald, H. *Colloids Surf., A* **2000**, *164*, 39−45.
(53) Ratto, T. V.; Longo, M. L. *Biophys. J.* **2002**, *83*, 3380−3392.
(54) Dubas, S. T.; Schlenoff, J. B. *Langmuir* **2001**, *17*, 7725−7727.
(55) Gao, C.; Leporatti, S.; Moya, S.; Donath, E.; Moehwald, H. *Langmuir* **2001**, *17*, 3491−3495.